

Experimental investigation of stress-strain curves in a cast TRIP steel under biaxial planar loading

K. Nagel¹, D. Kulawinski¹, S. Henkel¹, H. Biermann¹ and P. Hübner²

¹ TU Bergakademie Freiberg, Institute for Materials Engineering, Gustav-Zeuner-Straße 5, D-09599 Freiberg, Germany, kai.nagel@iwt.tu-freiberg.de

² University of Applied Sciences, Hochschule Mittweida (FH), Fachbereich Maschinenbau/Feinwerktechnik, Technikumplatz 17, D-09648 Mittweida, Germany

ABSTRACT. *This paper presents the characterization of the mechanical behavior of a recently developed metastable austenitic stainless cast steel under biaxial planar loading. Tests of different load ratios were carried out on cruciform specimens using a 250 kN biaxial servohydraulic tension-compression testing machine. Unloadings of 10 to 15 percent of the force were realized to obtain local elastic strains to determine the stresses in the gauge area of the specimens. Especially for the biaxial compression and the biaxial shear tests support plates have been developed to prevent buckling. Stress-strain curves of the two axes and equivalent von Mises stress-strain curves are discussed with uniaxial tensile and compression tests as reference to show the influence of biaxiality on the initial yield surface. Biaxial and uniaxial results show a good agreement to an isotropic material behavior of the cast TRIP steel. Scanning electron microscopy and electron backscatter diffraction imaging were applied to examine the development of the microstructure. The deformation-induced α' -martensite formation was detected in-situ with a ferrite sensor.*

INTRODUCTION

The real load state in a component in constructions is characterized in the general case by multiaxial loads. Usually a multiaxial stress state is approximately described with the aid of an equivalent stress or strain hypothesis to uniaxial material parameters, which can be easily and cost-saving determined. However, it is not possible to describe the material behavior for all load cases exactly with uniaxial parameters. Especially for efficient constructions as well as security-relevant components multiaxial tests are valuable additions.

The in-plane biaxial stress state is a special case of multiaxial loading. Thereby the direct biaxial test with cruciform specimens is the most realistic experimental test method to create a defined homogeneous in-plane biaxial stress state in flat sheets [1]. It is a general problem to estimate the stresses in the specimen from the applied forces. According to Lecompte et al. [2], material parameters are determined by the finite element method, in which boundary conditions and initial material parameters serve as basis for

the simulation. In this case, the real material parameters are determined by approximation of the measured and simulated results by iteration. The finite element method for the simulation of the effective bearing surface of the cruciform specimen in dependence on biaxial stress state was also used in the investigations of Granlund [3].

In this study the mechanical behavior of a recently developed metastable austenitic stainless cast TRIP steel is characterized under biaxial planar loading using cruciform specimens. The new cast transformation-induced plasticity (TRIP) steel is based on a high alloying concept using manganese to achieve excellent properties regarding strength and ductility [4]. Investigations on wrought alloys are predominantly published in the literature so far. The application of the recently developed high alloyed cast steel offers possibilities to reduce processing steps, production time and cost. If such steel is plastically deformed, the metastable austenite will transform into martensite. Jahn et al. [5] have compared different cast- and wrought alloys and found that there are no significant differences in the mechanical properties between the two production techniques.

EXPERIMENTAL DETAILS

Material

The investigated high alloyed material is a metastable austenitic stainless TRIP steel cast in plates by ACTech, Freiberg; Germany with a dimension of 340 mm x 340 mm x 10 mm. The ranges in the chemical composition between the various casts are given in Table 1. The plates were solution annealed under vacuum at 1050 °C for 30 minutes followed by subsequent quenching in high pressure helium atmosphere.

Table 1. Chemical composition of the high alloyed cast TRIP steel.

	Fe	C	Cr	Ni	Mn	Si
wt.%	bal.	0.03 - 0.05	15.3 - 15.9	5.7 - 6.4	5.8 - 6.4	0.8 - 1.0

Some uniaxial mechanical properties are summarized in Table 2. The yield stress, ultimate tensile strength and elongation at fracture were determined by uniaxial tensile tests according to DIN EN 10002 and Young's modulus by resonance method in accordance with DIN EN 843. A special feature of the new material is the high amount of strain hardening with high ultimate strength and elongation due to the TRIP effect.

Table 2. Mechanical properties of the high alloyed cast TRIP steel.

0.2 % yield stress, $R_{p0.2}$	198 MPa
Ultimate tensile strength, R_m	793 MPa
Elongation at fracture, A_5	47 %
Young's modulus, E	191 GPa

The microstructure is characterized by a dendritic solidification caused by the cast production route with coarse austenitic grains in the range of 0.1 - 1 mm. The castability of austenitic stainless steels can be improved by a small volume fraction of δ -ferrite, which is observed (lower than 3 %) in the interdendritic spaces and as well at grain boundaries of the austenite.

Testing method

Specifically for the applied static biaxial planar testing rig a flat and simple to manufacture specimen geometry was customized using FE simulations with the main aim to achieve a uniform stress and strain distribution in the central area of the cruciform specimen according to Gozzi [6]. Stress concentrations outside the center of the cross shaped specimen can be avoided as a result of the specimen design. The developed specimen geometry is given in figure 1a. The cast plates were milled to a uniform thickness of 5 mm and the specimen shape (332 mm x 332 mm x 5 mm) was cut by water jet.

The biaxial tests were conducted on a servohydraulic 250 kN biaxial tension-compression machine (Instron 8800). In this study the well-known problem of the stress calculation for biaxial testing with cruciform specimen was solved by using elastic unloading and reloading. The partial unloading method consists of three subsequent ramps. In the first one the specimens were loaded at stroke control in the range of 5 to 15 μm . Referring to the second ramp the specimens were elastically unloaded in force control with force reductions of 10 or 15 percent to avoid the backward deformation during unloading. Finally, the third ramp was used as force controlled reloading until the force achieved the value before unloading. The elastic ε_{el} and plastic ε_{pl} part of the total strain ε_{tot} in each axis was determined based on the data of the force and the strains measured by means of a biaxial orthogonal extensometer. Using fundamental equations for the plane stress condition the stress σ^* in each axis was calculated. It was necessary to estimate the equivalent stress σ_{eq} and equivalent true strain $\varepsilon_{true-eq}$ to describe the material behavior under biaxial loading to obtain the equivalent stress-equivalent true strain curve. In this study the von Mises yield criterion was adopted. The biaxial tests carried out are summarized in table 3. The tests were designed to get a load ratio $\lambda = 1$ or -1 where λ is the ratio of the loads in axes B and A, F_B and F_A , respectively. Due to the stroke control loading $|\lambda|$ varied between 0.9 and 1.2.

Table 3: Biaxial test program of the high alloyed cast TRIP steel.

Test	Load ratio $\lambda = \frac{F_B}{F_A}$	Support plates
Biaxial tension	1 (Realized: 0.90 ... 1.14)	No
Biaxial compression	1 (Realized: 0.99 ... 1.07)	Yes
Biaxial shear	-1 (Realized: -0.98 ... -1.22)	Yes

The development of supporting plates to prevent buckling of the specimen under compression was an aspect for biaxial compression and shear. The cruciform specimens were clamped into the developed supporting plates, see figure 1b. A teflon tape and teflon foil were attached to the plates to reduce the obvious friction between the plates and the specimen as much as possible. Due to the mounted supporting plates it was possible to realize every desired stress state and load ratio in the principal σ_1 - σ_2 -stress plane.

Uniaxial reference tests under compressive and tensile loading were performed on a servohydraulic testing system (100 kN MTS). The partial unloading method was also used for the uniaxial tensile tests according to the biaxial tests.

During the deformation the investigation of the transformation behavior of the metastable austenitic steel was recorded by using the commercially available ferrite sensor measuring device Fischer-scope MMS PC (Fischer GmbH) which was applied in the center at the surface of the cruciform specimen, as shown in figure 1b. As the measuring principle is based on the magnetic permeability only the ferromagnetic phases α' -martensite and δ -ferrite can be measured, whereas paramagnetic phases (e.g. austenitic γ -phase) are not detectable with this device. An accurate calibration of the ferrite sensor was achieved by four commercial standards of known ferrite content. According to investigations of Talonen et al. [7] and own studies the Fischerscope readings were multiplied by a factor of 1.7 to get the α' -martensite fractions.

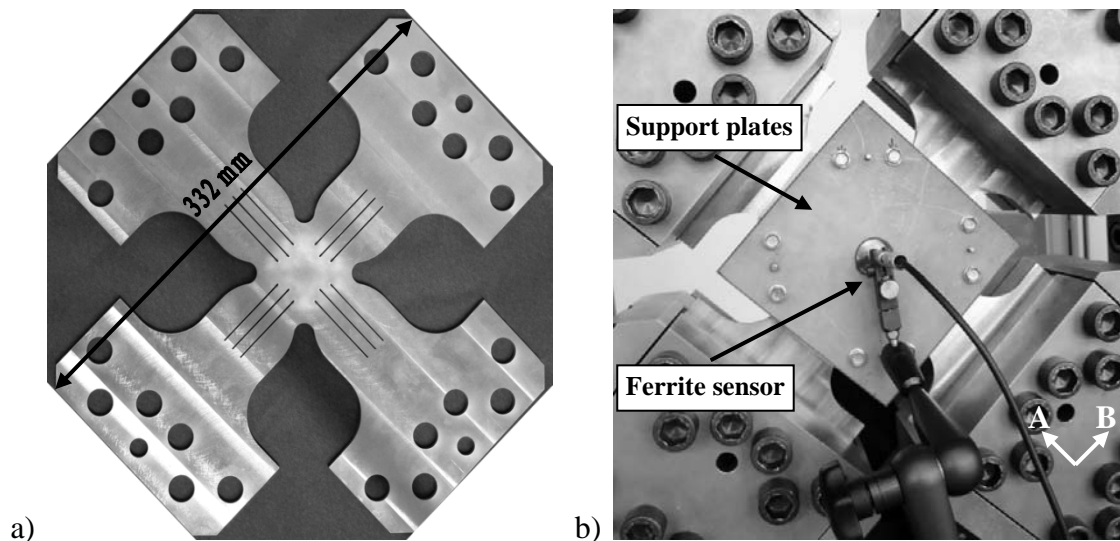


Figure 1: a) Developed cruciform specimen and b) Complete test set-up with support plates, ferrite sensor and biaxial orthogonal extensometer (on the backside).

After the biaxial tests samples were cut out from the center of the deformed specimen for further analysis. Scanning electron microscopy as well as electron backscatter diffraction (EBSD) measurements were used to examine the development of the microstructure. Samples were ground and electropolished for the EBSD measurements. Observations were carried out on a FEG-SEM LEO 1530 GEMINI at 20 kV acceleration voltage and the HKL Channel5 software was utilized.

EXPERIMENTAL RESULTS AND DISCUSSION

First an example of uniaxial tests is presented as a stress-true strain curve, see figure 2. The curves of the conventional true stress calculation ($\sigma_{\text{true}} = F/A$) and the partial unloading method (σ^*) are compared. An excellent agreement of the curves is achieved up to 1.5 % true strain. After this range the deviation between the two methods increases with strain. The result can be explained by the decrease of the material stiffness during plastic deformation. This effect is known in the forming of sheet metals and was investigated e.g. by Thibaud et. al. [8] and Schleich et. al. [9], who observed the change of the elastic material properties during deformation. It will be studied in more detail in future work. Nevertheless, our results show that the partial unloading method is appropriate for determination of the yield stress.

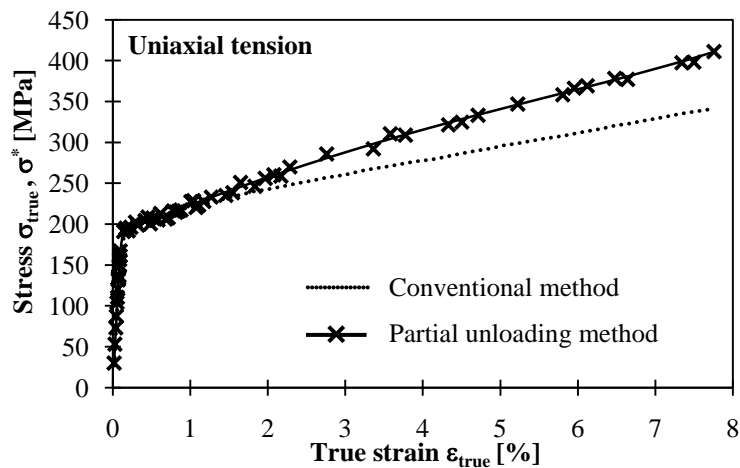


Figure 2: Comparison of different stress analyses on the basis of the stress-true strain curves of the high alloyed cast TRIP-steel.

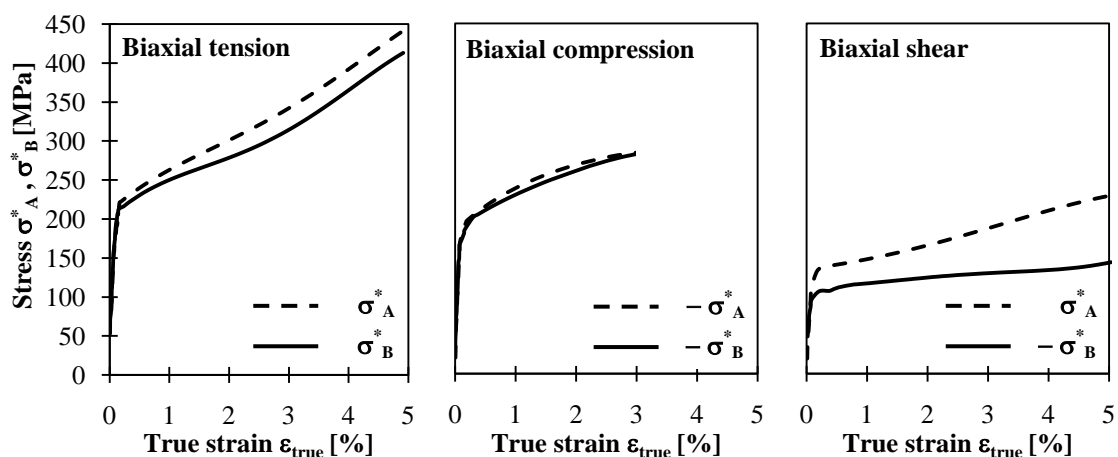


Figure 3: Stress-true strain curves in the two axes of the different biaxial tests.

The biaxial tests are first described in a flow curve for every single axis in figure 3. Results for the biaxial compression test are displayed only up to the beginning of buckling of the specimen. In this range an identical course was found. An improvement of the supporting plates to prevent buckling is planned with further tests. The stroke controlled loading is responsible for deviations of the stresses in the two axes.

According to the commonly used 0.2 % proof stress definition of yielding, the initial yield surface of the tests is given in figure 4. The investigated steel shows an initial yield surface which is described by the von Mises yield criterion very well. This indicates an almost isotropic material behavior. The determined yield stresses of the biaxial tensile test and the uniaxial compressive tests are within the scatter slightly higher than the values of the uniaxial tensile test and the biaxial shear test, which needs to be verified by further investigations. The yield stresses of the uniaxial tests and the values of the two axes as well as the equivalent von Mises yield stresses of the biaxial tests are given in table 4. Generally, all tests show an equivalent yield stress in the range of 214 MPa.

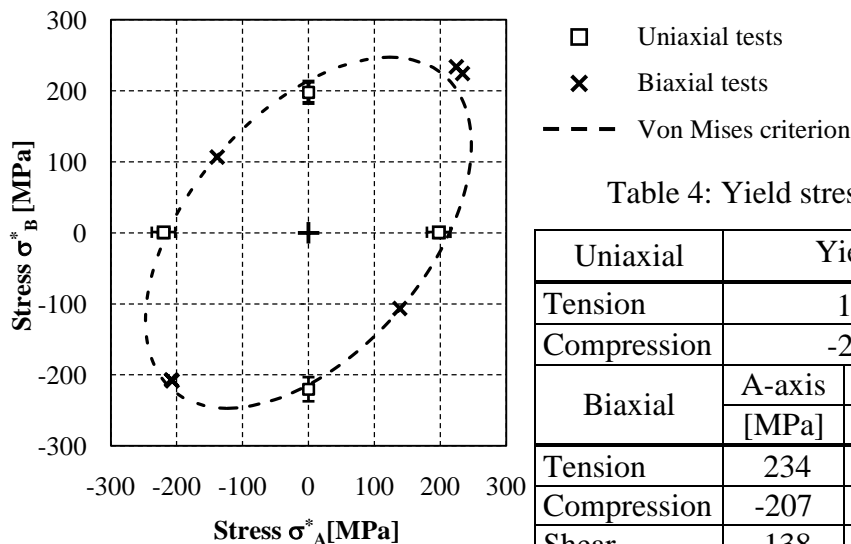


Figure 4: Initial yield surface.

Table 4: Yield stresses of the tests.

Uniaxial	Yield stress $R_{p0.2}$		
Tension	198 ± 15 MPa		
Compression	-220 ± 18 MPa		
Biaxial	A-axis	B-axis	$\sigma_{\text{von Mises}}$
	[MPa]	[MPa]	[MPa]
Tension	234	224	229
Compression	-207	-208	208
Shear	138	-107	213

Figure 5a shows the equivalent stress-true equivalent strain curves based on the partial unloading method. After achieving the yield stress a strong strain hardening of the material is identified along with the martensitic transformation of the metastable austenite.

The start of yielding (Fig. 5a) of the steel agrees with the initiation of the deformation induced martensite transformation (Fig. 5b). This martensite development in the presently investigated case is comparable to the commonly described results of uniaxial deformation [10]. The different martensite evolutions for the separate tests can be attributed to variations of the chemical composition in the several cast plates and will be studied in more detail in the future.

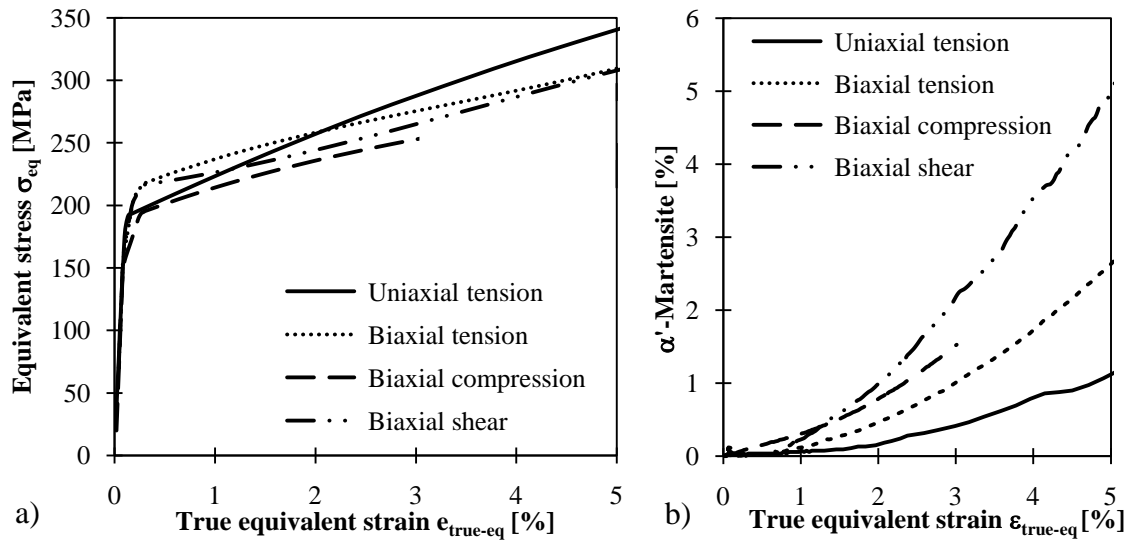


Figure 5: a) Equivalent von Mises stress-strain curves and b) Martensite evolution subjected to the true equivalent strain.

Deformed cruciform specimens have been examined in terms of scanning electron microscopy and EBSD measurements to gain information about the development of the microstructure. A characteristic micrograph for the tests is displayed by the biaxial compression sample deformed to a compressive equivalent true strain of approximate 8 % in figure 6. The SEM micrograph shows the typical arrangement of several deformation bands in the material as also observed in uniaxial tests [11]. The martensite transformation is shown in the EBSD pattern, see figure 6b. Initially the metastable austenite phase transforms into regions inside the deformation bands, which are indexed as a hexagonal phase by EBSD. These regions subsequently transform into α' -martensite with increasing deformation as described in detail by Olson and Cohen [10].

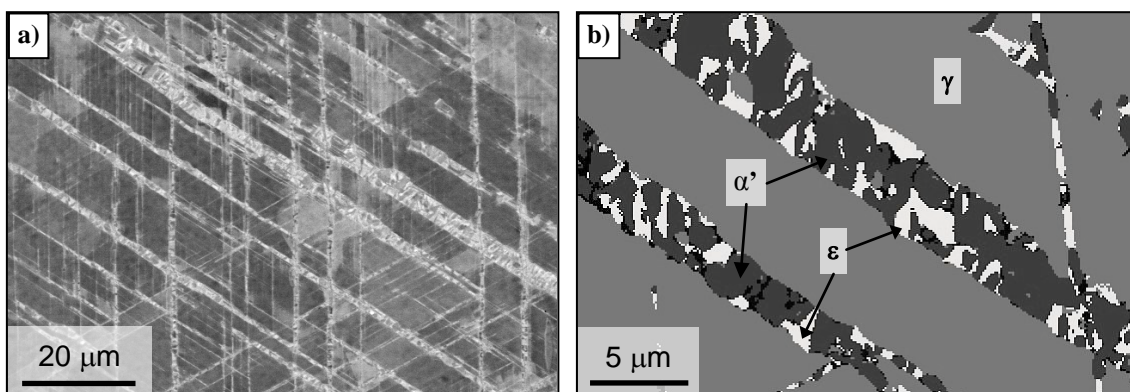


Figure 6: Microstructure of the high alloyed cast TRIP steel after biaxial compression. a) SEM micrograph in backscattered electron contrast and b) EBSD phase map; white: hexagonally indexed phase (ϵ -Fe dataset); bright grey: γ -austenite; dark grey: α' -martensite. (black color is zero solution)

SUMMARY AND CONCLUSIONS

The description of the mechanical behavior of the metastable austenitic cast TRIP steel under biaxial planar loading is successfully carried out by using the partial unloading method to determine the stress-strain curve. This is experimentally verified by the comparison of uniaxial tensile and biaxial tests. By the use of the developed supporting plates any possible stress state and load ratio can be adjusted in the principal σ_1 - σ_2 -stress plane. Unexplained effects like the decreasing stiffness in dependence of the plastic strain and differences between flow curves will be studied in further tests.

It is remarkable, that the investigated cast material with its coarse grains also shows an almost isotropic initial yielding behavior and a significant TRIP-effect. Metallographic investigations and in-situ ferrite sensor measurements agree with the well-known austenite-martensite transformation behavior. The start of martensitic transformation by achieving the yield stress is a special feature of the investigated cast material.

ACKNOWLEDGMENTS

The authors would like to thank all of the involved staff of the collaborative research centre SFB 799 and the Deutsche Forschungsgemeinschaft (DFG) for financial support.

REFERENCES

1. Demmerle, S. and Boehler, J.P. (1993) *J. Mech. Phys. Solids* **41**, 143-181.
2. Lecompte, D. et al. (2007) *Int. J. Solids Structures* **44**, 1643-1656.
3. Granlund, J. (1997). PhD Thesis, Luleå University of Technology - Department of Civil and Mining Engineering, Sweden.
4. Weiß, A.; Gutte, H.; Radke, M. and Scheller, P. (2008). *Patent publication WO002008009722A1*.
5. Jahn, A.; Kovalev, A.; Weiß, A.; Scheller, P.R.; Wolf, S.; Krüger, L.; Martin, S. and Martin, U. (2009). In *Proc. of ESOMAT 2009*, eds. P. Sittner, L. Heller, V. Paidar, published by EDP, Sciences (www.esomat.org), paper 05013, DOI:10.1051/esomat/200905013.
6. Gozzi, J.; Olsson, A. and Lagerqvist, O. (2005) *Exp. Mechanics* **45** (6), 533-540.
7. Talonen, J.; Apegren, P. and Hänninen, H. (2004) *Mater. Sci. Technol.* **20**, 1506-1512.
8. Thibaud, S.; Boudeau, N. and Celin, J. C. (2004) *Int. J. Damage Mechanics* **13**, 107-122.
9. Schleich, R. et al. (2007) *Mat.-wiss. u. Werkstofftech.* **38** (10), 872-877.
10. Olson, G. and Cohen, M. (1975) *Metall. Trans. A* **6**, 791-795.
11. Martin, S.; Wolf, S.; Martin, U.; Krüger, L. and Jahn, A. (2009). In *Proc. of ESOMAT 2009*, eds. P. Sittner, L. Heller, V. Paidar, published by EDP, Sciences (www.esomat.org), paper 05022, DOI:10.1051/esomat/200905022.